

3D Printing Feedstocks from Recycled Materials

Nicole E. Zander and Margaret Gillan, U.S. Army Research Laboratory, Weapons and Materials Research Directorate, Aberdeen Proving Ground, Aberdeen, MD

Abstract

United States Army warfighters in theater are often faced with the challenge of broken, damaged, or missing parts necessary to maintain the safety and productivity required. Waste plastics can be utilized to improve the self-reliance of warfighters on forward operating bases by cutting costs and decreasing the demand for the frequent resupplying of parts by the supply chain. In addition, the use of waste materials in additive manufacturing in the private sector would reduce cost and increase sustainability, providing a high-value output for used plastics. Experimentation is conducted to turn waste plastics into filament that can be used in fused deposition modeling. The effect of extrusion temperature and number of extrusion cycles on polymer viscosity and crystallinity are explored. The effect of blends and fillers to impart additional functionality are also examined. Tensile specimens were tested and compared to die-cut and injection molded parts. Parts printed from recycled polyethylene terephthalate had the highest tensile strength of all recycled plastics evaluated (35.1 ± 8 MPa), and were comparable to parts printed from commercial polycarbonate-ABS filament. Elongation to failure of all recycled plastics was similar to their injection molded counterpart. In addition, select military parts were printed with recycled filament and compared to original parts. This research demonstrates some of the first work on the feasibility of using recycled plastic in additive manufacturing.

Introduction

Additive manufacturing (AM) is a type of manufacturing process that builds custom products, generally in a layer-by-layer fashion, from a three dimensional (3D) computer-aided design (CAD) model. Plastics, metals, ceramics, composite and even biological materials can be joined in this fashion to generate 3D objects [1-3]. The potential applications of AM technologies are extensive—everything from pre-production models and temporary parts to end-use aircraft parts and medical implants [4]. AM offers many advantages over traditional manufacturing, including increased part complexity and reduced time and cost for one-off items [5,6]. This greatly enables new product development and drastically reduces the time from production to market [7,8]. While AM offers many important advantages, there are several challenges, including slow build rates, high production costs for scale up, post-processing requirements, limited build volumes,

poor mechanical properties, and lack of industry standards for testing and evaluation [9,10].

Fused deposition modeling is one of the most cost-effective AM methods, with desktop printers costing as low as a few hundred dollars. However, the range of materials commercially available is limited to a handful of polymers including ABS, PLA, Nylon, and Polycarbonate with bulk strengths between 30-100 MPa and elastic moduli on the order of 1.3 – 3.6 GPa [11]. Printed parts have substantially reduced strengths due to voids and weak interlayer adhesion [11]. While many polymers used for bottles and packaging have bulk strengths below the aforementioned range, polyethylene terephthalate (PET) has an average strength and modulus of 70 MPa and 3.1 GPa, respectively [12]. Polypropylene (PP) and polystyrene (PS) have average tensile strengths of 40 and 50 MPa, respectively [13,14]. While currently there is no commercial neat or recycled PET or recycled PP or PS FDM feedstocks, based on the mechanical properties, they may be suitable materials. Virgin polyethylene terephthalate (PET) is one of the most widely used and important engineering plastics. It is used in many applications such as in food and liquid packaging materials, electronic equipment, automotive products and power tools. In addition to excellent tensile, impact strength, and clarity, it also has reasonable thermal stability [15]. The total global consumption has more than doubled from 23.6 million tons in 2005 to 54 million in 2010, and a 4.5% growth rate per year is expected [16,17]. PET bottles are also widely available on forward operating bases, where the average warfighter discards nearly 300 pounds of PET per year [18].

Recently, there has been interest in reusing recycled plastics in value added processes such as in the production of fibers and 3D printing filaments. Shin and Chase, and Zander et. al. formed electrospun fibers from Styrofoam and bottle-grade PET, respectively [19-21]. Rajabinejad et. al., and Zander et. al. generated melt-spun fibers from bottle-grade PET and blends with other recycled polymers, respectively [22,23]. A handful of companies now sell commercial filament made from recycled plastics such as recycled ABS filament from Kick Fly[®] and recycled PET (chemically modified PET, 90% recycled content) from Refil[®]. Even though some studies have focused on recycled materials, there is currently minimal published work on using 100% recycled polymers for fabrication of 3D printable filament.

In this work, FDM filament was generated from 100% recycled PET, PP and PS from bottles and packaging

without any chemical modifications or additives. The effect of plastic source, drying, and processing conditions on the thermal, rheological and mechanical properties were evaluated. Recycled PET (rPET) was shown to be a viable new feedstock for FDM, with mechanical properties of printed parts comparable to parts made from commercial filament. In addition to small parts for evaluation, select larger long lead item military parts were also printed with the filament

Materials

Polymer Filament Fabrication

Polymer filament was prepared by rinsing plastic containers with ethanol, drying and cutting into pieces that could be fed either through a cross-cutting paper shredder (rPET, recycled high density polyethylene (rHDPE) and recycled polypropylene (rPP)) or a high speed blender (recycled polystyrene (rPS)). After shredding, rPET, rHDPE and rPP was further processed by mixing in a high speed blender to form uniform shred sizes. Carbon nanofibers (Pyrograf, PR-19-XT-LHT) were also blended with rPET to make a composite filament. Blends were mechanically mixed before feeding into extruder. Shredded polymer was fed into a Process 11 Parallel Twin-Screw Extruder (Thermo Fisher) in conveying mode at temperatures ranging from 165 °C to 260 °C to melt the polymers and the extrudate collected on a belt and/or spooler (Filabot). Nozzle diameter was adjusted between 2.5 mm and 3.0 mm to account for die swell and shrinkage (target diameter was 3.0 mm). In addition, filament was also made from virgin PET pellets for reference. The shredded rPET, rHDPE and rPP did not feed uniformly into the extruder and consequently, filament diameter was not well controlled. Consolidating the polymer, pelletizing and extruding a second time proved the best method to generate uniform filament diameters. Figure 1 displays images of the rPET shreds, pellets after the first extrusion, and the filament from the second pass.



Figure 1. Optical images of recycled polyethylene terephthalate, (A) shredded, (B) pelletized, (C) filament.

3D Printing of Polymer Filament

Recycled and virgin PET filament was dried overnight at RT under vacuum before use. Filament was printed into tensile bars (Type V, ASTM D638) on a Taz 6 FDM printer. For comparison, PET filament from commercial PET pellets and polycarbonate-acrylonitrile butadiene styrene (PC-ABS) filament were printed. STL files were imported into Simplify 3D for editing. The bed temperature was varied between 30 °C and 100 °C, while

the nozzle temperature was varied between 220 °C and 270 °C. The build orientation was in the Y direction (flat, direction of pull in tensile test), with layer height set to 0.2 mm.

Tensile bars were also cut from plastic containers using a punch press (Type C, ASTM D412). Injection molded samples were prepared from cleaned, shredded and dried recycled plastic as previously described on the Xplore® Microcompounder (MC15). The polymer was melted at 260 °C and injected into a mold (Type V, ASTM D638) set at 65 °C with a pressure of 6 bar.

Characterization

Chemical analysis was performed by Fourier transform infrared-attenuated total reflectance (FTIR-ATR) (Thermo Nicolet Nexus 870 ESP) using 256 averaged scans and 4 cm⁻¹ resolution over a range of 4000 - 400 cm⁻¹.

Thermal properties were measured using differential scanning calorimetry (DSC) with a heat/cool/heat program (Discovery DSC, TA Instruments). All samples were heated at a rate of 20 °C per min to 300 °C, cooled at 20 °C per min to -50 °C, and then heated again at 20 °C per min to 300 °C. DSC data was processed using TRIOS software (TA Instruments). Crystallization was calculated using the following equation:

$$\% \text{ crystallinity} = (\Delta H_m - \Delta H_{cc}) / \Delta H_f ;$$

where ΔH_m is the area under the melting endotherm, ΔH_{cc} is the area under the cold crystallization/ recrystallization curve, and ΔH_f is the heat of fusion for a 100 % crystalline sample (PET: 140 J/g, PP: 207 J/g, polyethylene: 293 J/g) [24].

Thermal mechanical properties were probed in the single cantilever mode using dynamic mechanical analysis (DMA, Q800 TA Instruments). Temperature sweeps from 25 °C to 200 °C at 2 °C per min were conducted at a frequency of 1.0 Hz. Amplitude was set to 200 μ m. Sample dimensions were 35 mm x 12.5 mm x 2 mm for DMA bars and 35 mm x 2.5 mm x 2.5 mm for filament. Thermogravimetric analysis (TGA) was conducted on a Q5000 (TA Instruments) on filament. All samples were heated at 20 °C per min to 800 °C under nitrogen.

Rheological experiments were conducted on an AR2000 rheometer (TA Instruments) at 270 °C. 25 mm aluminum plates were used. A shear rate of 1 s⁻¹ was applied with a ramp from 0.1 to 100.

Uniaxial tensile experiments were conducted at a strain rate of 0.0009 mm/s and 0.004 mm/s for the die-cut and printed/injection molded specimens, respectively on a servohydraulic Instron model 5000R test machine with 2 kN grips. A low capacity (5 kN) load cell was used since the anticipated loads were relatively small. A DIC system was used to obtain displacement/strain data. The system comprised of one 1 megapixel monochrome digital camera (Point Grey) that streamed images (2-10 frames per second) directly to a computer. To prepare the

specimens for DIC, the samples were painted with white spray paint and then speckled with black spray paint. The morphology of the broken tensile specimens were probed using a field-emission scanning electron microscope (SEM, Hitachi S-4700) after sputter coating with gold-palladium.

Results

Recycled polymers have a variety of different additives, fillers and dyes, and may have experienced different processing conditions, even for the same polymer type. To get a better understanding of different recycled polymer feedstocks and the best properties to expect from such materials, thermal and mechanical testing was performed. Tensile dogbones were cut using a die out of milk jugs, soda bottles, and yogurt containers, and shredded polymers were also injection molded. Polystyrene materials were too brittle to punch out. Representative stress-strain curves are displayed in Figure 2. The soda bottles (PET) had the highest tensile strength, nearly 5 times that of the polyolefin materials (PP, PE). The rPET bottles had yielding followed by strain hardening, with a significant amount of stretching before failure. Figure 3 displays representative stress-strain curves for 3D printed tensile bars. The tensile strength of printed rPET was nearly twice that of rPS and rPP (35.1 ± 8 vs. 19.9 ± 3.9 and 20.1 ± 2.3 MPa), and comparable to virgin PET and PC-ABS (28 ± 9 and 37.0 ± 2 MPa). Elongation to failure of rPET was similar to injection molded rPET (3.5 vs. 3.2 %). Recycled PP printed samples had a longer elongation to failure compared to injection molded samples. HDPE filament has not successfully been extruded due to its high viscosity.

A cross-section of a fractured rPET tensile bar is displayed in Figure 4, along with printed tensile bars and a lodge projectile removal tool (LPRT) long lead item part printed with rPET filament. The cross-section is nearly solid and differentiation of printed roads is difficult, and the commonly seen printing defects between layers are not present throughout the part. The fracture surface is characteristic of thermoplastic ductile fracture, with some crazes generated by tear fractures during deformation of the polymer. The LPRT part conformed to fit and function, but was not evaluated quantitatively due to lack of proper test fixture.

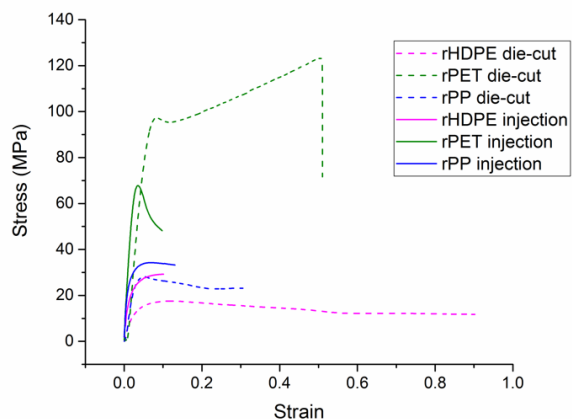


Figure 2. Representative stress-strain curves of die-cut and injection molded recycled polymers.

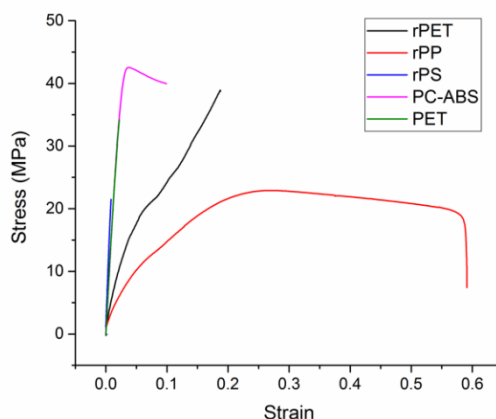


Figure 3. Representative stress-strain curves of 3D printed recycled and virgin polymers.

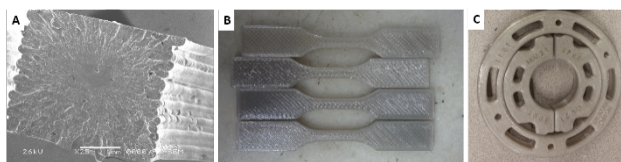


Figure 4. Scanning electron microscopy and optical images of recycled polyethylene terephthalate (PET). (A) Fracture surface of 3D printed tensile bar, (B) 3D printed tensile bars, (C) 3D printed lodge projectile removal tool (LPRT).

Chemical characterization was performed using FTIR (Figure 5). The two sources of PS examined (petri dishes and utensils (opaque)) appear chemically identical, even with the presence of fillers in the utensil. The two sources of PET (water and soda bottles) also appear identical. The PP cups and yogurt containers had three regions that were notably different, most likely due to the dyes in the yogurt containers.

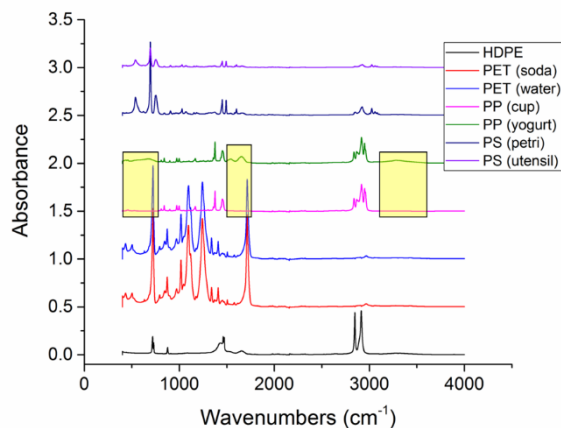


Figure 5. Chemical characterization of recycled polymers using FTIR-ATR. Yellow boxes highlight different peaks between polypropylene sources.

Table 1 displays thermal properties from DSC measurements. The two sources of rPP examined, PP cups and yogurt containers, have the same melting temperature and similar percentages of crystallinity, but the crystallization temperatures are 16 degrees apart. This difference may be due to the dyes and fillers in the yogurt container compared to the cups which were transparent and likely had less additives. The thermal characterization of rPS only provided glass transition (T_g) information since it is an amorphous polymer, and the T_g s were more or less identical for the two sources of PS. The rPET in the soda bottles had a higher crystallization temperature compared to water bottles, and was more crystalline. Only one source of rHDPE was examined.

Table 1. Thermal characterization of recycled polymers using differential scanning calorimetry.

Polymer	T_g (°C)	T_c (°C)	T_m (°C)	% Crystallinity
rPP (cup)	-6.8	126.6	165.9	53.6
rPP (yogurt tub)	*	110.7	169.9	45.7
rPS (utensil)	91.7			
rPS (petri dish)	89.2			
rPET (soda bottle)	66.5	188.2	248.4	23.1
rPET (water bottle)	73.3	154.72	250.1	17.9
rHDPE (milk bottle)	**	115.6	137.8	75.5

* T_g not visible, ** T_g below instrument minimum (< -80 °C)

Blends of recycled polymers were also prepared with and without a styrene ethylene butylene styrene (SEBS) compatibilizer. Blends with rHDPE did not print well due to the high viscosity and shrinkage during cooling. The rPS/rPET blend yielded a very brittle material that broke in the print head. Recycled PET and rPS blends with rPP were the most promising and could be printed. In addition, the filament was less brittle than the rPET filament and could be more easily handled. Figure 4 displays the storage modulus of printed DMA bars. G' was similar for neat rPET and the 50-50 blend. The storage modulus dropped significantly for other blend compositions (25-75) and was more similar to neat rPP.

The glass transition (T_g) determined from the maximum of the tan delta peak temperature also changed with blend composition (data not shown). The T_g for the 50-50 blend was similar to rPET (82.9 vs. 84.2 °C), but it was shifted to higher temperatures for the 25-75 and 75-25 blends (85.8 and 86.7 °C, respectively).

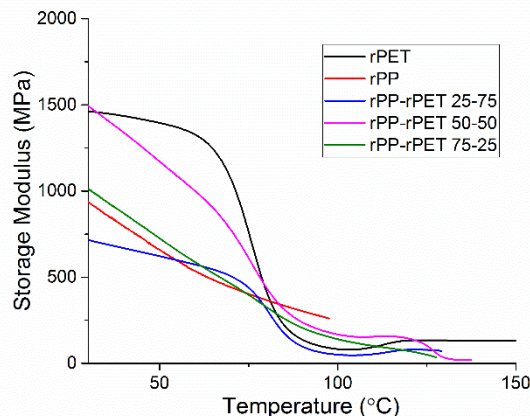


Figure 4. Dynamic mechanical analysis of recycled polymer blends.

Rheological analysis of the rPET-rPP 50-50 blend is displayed in Figure 6. The zero shear viscosity was highest for the blend compatibilized with SEBS-maleic anhydride (SEBS-MA), which could be due to intermolecular interactions between the end groups of PET and the maleic anhydride functionalities. The zero shear viscosity compatibilized with unfunctionalized SEBS was lower than the uncompatibilized blend.

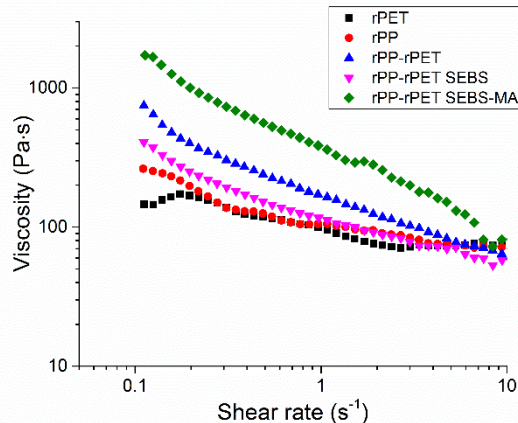


Figure 6. Rheological behavior of recycled PP-PET 50-50 blends.

The effect of a reinforcing agent on rPET was also evaluated. Carbon nanofibers (CNF) were added to rPET at concentrations of 5 and 7.5 wt. % and mixed in the

extruder. A significant increase in the viscosity was observed for the filled polymer, but the difference between 5 and 7.5 wt. % was not significant (data not shown). A marked increase in the storage modulus and glass transition temperature was observed for the samples wt. 7.5 wt. % CNF, likely due to greater confinement of the amorphous segments of the polymer (Figure 7). Tensile testing of 3D printed tensile bars yielded similar results to neat rPET (38.7 ± 8 MPa for rPET / 7.5 wt. % CNF vs. 35.1 ± 8 MPa for rPET).

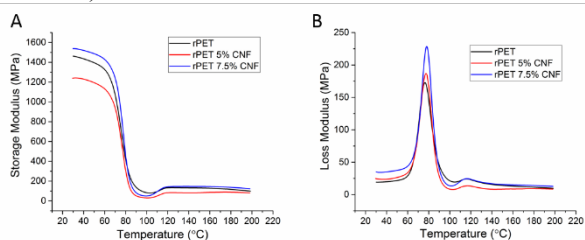


Figure 7. Dynamic mechanical analysis of recycled PET reinforced with carbon nanofibers. (A) Storage modulus, (B) Loss modulus.

Discussion

In this work, the use of recycled PET, PP, PS and HDPE as new feedstock materials for FDM was evaluated. While these polymers are commonly used in many applications, they are not widely utilized as feedstocks for FDM due a variety of reasons including water absorption (PET), crystallinity, and warpage, which can make printing difficult. Recycled polymers may contain contaminants and processing aids, and have likely been subjected to several thermal and mechanical stresses during processing cycles, potentially leading to lower performance than a virgin part. However, injection molded rPET has a similar tensile strength to virgin material and is in the range of the polymers commonly used in FDM (68 vs 55 MPa) [25]. Thus it was hypothesized that parts printed from rPET could be at least comparable to parts made with COTS filament such as PC-ABS, and indeed this was the case.

Crystallization can have a large impact on the performance of the resulting part. Barrier properties, flexibility, and sometimes optical clarity are required for container and bottles. Stretching during the molding cycle may be compromised if the crystallinity is too high. On the other hand, if the crystallinity is too low, mechanical performance and barrier properties can be reduced. The crystallinity varied slightly between the different sources of the polymers, with clear PP cups having higher crystallinity than PP containers with fillers such as colorants. It is likely the fillers interfered with the crystallization process. Soda bottles also had higher crystallinity than water bottles, possibly due to the thicker wall thickness of the former and slower cooling.

Dynamic mechanical analysis of rPET-rPP blends revealed that the glassy modulus at 30 °C was

similar for rPET and the 50-50 blend, and ca. 1.5-2 times that of the other blends and rPP. The T_g was shifted higher for the 25-75 and 75-25 blends, seemingly counterintuitive to the rule of mixtures. Possibly, the immiscible PP phase restricted the motion of the amorphous segments of the PET polymer. Further research is needed to investigate why this was not observed in the 50-50 blend. In addition, evaluation of tensile properties would be useful to determine if the 50-50 blend can match the tensile strength of rPET, but increase elongation and yield a less brittle material.

The effect of a reinforcing filler on rPET was also examined. Carbon nanofibers were blended into rPET at 5 and 7.5 wt. % loading. The addition of 5 wt. % CNF resulted in a decrease in the storage modulus, possibly due to agglomeration. The T_g of the polymer was slightly increased, along with the height of the loss peak increased. The addition of 7.5 wt. % showed a significant increase in storage modulus in both glassy and rubbery regimes, and also T_g . Based on DMA results, it was expected that the tensile strength of the rPET loaded with 7.5 wt. % CNF would show an increase in strength, but the modest increase was not statistically significant. This may be due to the likely weak interface between the fibers and the polymer chains, and surface modification of the CNF could improve interfacial interactions. Additional work in filler modification and evaluation of higher loading conditions is warranted.

In conclusion, recycled PET has been shown to be a suitable material for FDM printing, provided the material is properly cleaned and dried. While printed parts achieved only approximately half the tensile strength of their injection molded counterpart, tensile strength was equivalent to printed parts made from COTS PET pellets and commercial PC-ABS filament. In addition, as a proof-of-concept, the LPRT long-lead item part was printed using the rPET filament and had good fit and function. Future work will involve testing select 3D printed long-lead parts against original parts to determine if they could be a suitable long-term or at least temporary replacement. The use of additives such as nucleation agents and chain extenders, or fillers such as toughening agents, may further improve the mechanical properties of the rPET filament and expand the realm of applications in which it can be used.

References

1. W.E. Frazier, *J. Mater. Eng. Perform.*, **23**, 1917 (2014)
2. F.P.W. Melchels, M.A.N. Domingos, T.J. Klein, J. Malda, P.J. Bartolo, and D.W. Huttmacher, *Prog. Polym. Sci.*, **37**, 1979 (2012).
3. G.G. Levy, R. Schindel, and J.P. Kruth, *CIRP Ann. Manuf. Technol.*, **52**, 589 (2003).
4. J. Gardan, *Int. J. Prod. Res.*, **54**, 3118 (2016).
5. S.H. Huang, P. Liu, A. Mokasdar, and L. *Int. J. Adv. Manuf. Technol.*, **67**, 1191 (2013).

6. B.P. Conner, G.P. Manogharan, A.N. Martof, L.M. Rodomsky, C.M. Rodomsky, D.C. Jordan, and J.W. Limperos, *Addit. Manuf.*, **1-4**, 64 (2014).
7. P. Lein, *Defense Systems Information Analysis Center*, **2**, Spring (2015).
8. Academy of Aerospace Quality, Advantages and Limitations of Additive Manufacturing, http://aaq.eng.auburn.edu/drupal7/AdditiveManufacturing_Introduction (accessed 10/17/17).
9. American Composites Manufacturers Association, Pros and Cons of Additive Manufacturing, <http://compositesmanufacturingmagazine.com/2014/10/pros-cons-additive-manufacturing/2/>, 2015 (accessed 10/17/17).
10. Y. Huang, M.C. Leu, J. Mazumder, and A. Donmez, *Journal of Manufacturing Science and Engineering*, **137**, 014001 (2015).
11. W.C. Smith, and R.W. Dean, *Polymer Testing*, **32**, 1306 (2013).
12. <https://www.matbase.com/material-categories/natural-and-synthetic-polymers/thermoplastics/engineering-polymers/material-properties-of-polyethylene-terephthalate-bottle-grade-pet-bottle-grade.html#mechanical-properties> (accessed 11/30/17).
13. <https://www.shimadzu.com/an/industry/petrochemicalchemical/i201.html> (accessed 12/6/17).
14. <http://www.matweb.com/search/datasheettext.aspx?matguid=5f099f2b5eeb41cba804ca0bc64fa62f> (accessed 12/6/17).
15. F. Awaja, and D. Pavel, *Eur. Polym. J.*, **41**, 1453 (2005).
16. G. Karayamidis, D. Archilias, *Macromol. Mater. Eng.*, **292**, 128 (2007).
17. IHS WP Report: Polyethylene Terephthalate (PET), <http://www.sriconsulting.com/WP/Public/Reports/pet/>, 2011 (accessed 10/17/17).
18. S.D. Cospers, H.G. Anderson, K. Kinnevan, and B.J. Kim, *US Army Corps of Engineers Report*, **TR-13-17** (2013).
19. C. Shin, and G.G. Chase, *Polym. Bull*, **55**, 209 (2005).
20. C. Shin, *J. Colloid Interface Sci.*, **302**, 267 (2006).
21. N.E. Zander, M. Gillan, and D. Sweetser, *Materials*, **9**, 247 (2017).
22. H. Rajabinejad, R. Khajavi, A. Rashidi, N. Mansouri, and M.E. Yazdanshenas, *Int. J. Environ. Res.*, **3**, 663 (2009).
23. N.E. Zander, M. Gillan, and D. Sweetser, *Materials*, **10**, 1044 (2017).
24. W.J. Sichina, http://www.perkinelmer.com/Content/applicationnotes/app_thermalcrystallinitythermoplastics.pdf, 2000 (accessed 11/30/17).
25. <http://www.matweb.com/reference/tensilestrength.aspx> (accessed 11/30/17)